

# Global Transcriptional and Physiological Responses of Saccharomyces cerevisiae to Ammonium, L-Alanine, or L-Glutamine Limitation

**Usaite, Renata; Patil, Kiran Raosaheb; Grotkjær, Thomas; Nielsen, Jens; Regenberg, Birgitte**

*Published in:*
Applied and Environmental Microbiology

*Link to article, DOI:*
10.1128/AEM.00548-06

*Publication date:*
2006

*Document Version*
Publisher's PDF, also known as Version of record

APPLIED AND ENVIRONMENTAL MICROBIOLOGY, Sept. 2006, p. 6194–6203 Vol. 72, No. 9
0099-2240/06/$08.00+0 doi:10.1128/AEM.00548-06


# Global Transcriptional and Physiological Responses of *Saccharomyces cerevisiae* to Ammonium, L-Alanine, or L-Glutamine Limitation†

Renata Usaite,[1] Kiran R. Patil,[1] Thomas Grotkjær,[1] Jens Nielsen,[1]* and Birgitte Regenberg[1,2]

*Center for Microbial Biotechnology, BioCentrum-DTU, Technical University of Denmark, Kgs. Lyngby, Denmark,[1] and Institute of Molecular Biosciences, Johann Wolfgang Goethe University, Frankfurt am Main, Germany[2]*

Received 7 March 2006/Accepted 4 July 2006

**The yeast *Saccharomyces cerevisiae* encounters a range of nitrogen sources at various concentrations in its environment. The impact of these two parameters on transcription and metabolism was studied by growing *S. cerevisiae* in chemostat cultures with L-glutamine, L-alanine, or L-ammonium in limitation and by growing cells in an excess of ammonium. Cells grown in L-alanine-limited cultures had higher biomass yield per nitrogen mole (19%) than those from ammonium-limited cultures. Whole-genome transcript profiles were analyzed with a genome-scale metabolic model that suggested increased anabolic activity in L-alanine-limited cells. The changes in these cells were found to be focused around pyruvate, acetyl coenzyme A, glyoxylate, and α-ketoglutarate via increased levels of *ALT1*, *DAL7*, *PYC1*, *GDH2*, and *ADH5* and decreased levels of *GDH3*, *CIT2*, and *ACS1* transcripts. The transcript profiles were then clustered. Approximately 1,400 transcripts showed altered levels when amino acid-grown cells were compared to those from ammonium. Another 400 genes had low transcript levels when ammonium was in excess. Overrepresentation of the GATAAG element in their promoters suggests that nitrogen catabolite repression (NCR) may be responsible for this regulation. Ninety-one genes had transcript levels on both L-glutamine and ammonium that were decreased compared to those on L-alanine, independent of the concentration. The GATAAG element in these genes suggests two groups of NCR-responsive genes, those that respond to high levels of nitrogen and those that respond to levels below 30 μM. In conclusion, our results reveal that the nitrogen source has substantial influence on the transcriptome of yeasts and that transcriptional changes may be correlated to physiology via a metabolic model.**

In its natural habitat, the yeast *Saccharomyces cerevisiae* is often growth limited by the availability of nitrogen (1, 37). To survive and adapt to various environmental conditions, *S. cerevisiae* has evolved complex regulatory networks to ensure an efficient regulation of metabolism, as illustrated by the systems for sensing and regulation of the nitrogen metabolism (7, 13, 20). An example of global response to amino acid depletion is the transcriptional induction of amino acid biosynthesis genes by the transcription factor Gcn4 (20). Additional specific systems are responsible for the sensing of amino acids or ammonium in the medium and the subsequent induction of corresponding transporter genes and pseudohyphal growth (13, 16, 22, 27, 30).

Central for the transcriptional regulation of nitrogen as well as carbon metabolism are the target of rapamycin (TOR) pathway and the protein kinase A pathway. These pathways control the metabolism by sequestering transcription factors such as Msn2, Msn4, Gln3, and Crf1 to the cytosol when nutrients are in excess (4, 31, 49). When glucose is depleted from the medium, Msn2 and Msn4 enter the nucleus, where they induce transcription of tricarboxylic acid (TCA) cycle genes, gluconeogenesis genes, and genes carrying the stress response element STRE (40). The same is the case for Gln3, which enters the nucleus upon inactivation of the TOR pathway or a change in the nitrogen availability, where it induces genes with the GA TAAG promoter element (4). Moreover, Gln3 is part of a network involved in nitrogen catabolite repression (NCR), which ensures selective use of different available nitrogen sources (7). This selection is obtained by transcriptional repression and induction of genes involved in nitrogen uptake and metabolism, such as *GLN1*, *GDH2*, *GLT1*, and *GAP1* (7, 8, 32, 43). NCR is dependent on at least four transcription factors that compete for the *cis*-acting element GATAAG (7). Two GATA transcription factors, Gln3 and Gat1, are transcriptional activators, while Dal80 and Gzf3 function as transcriptional repressors (10, 11, 32, 43, 46). The TOR pathway has been shown to trigger NCR upon increased levels of intracellular L-glutamine (28), though the link is probably not direct, as different nitrogen sources, such as ammonium and L-glutamine, are shown to repress different sets of NCR-sensitive genes (43). Part of this complexity is probably due to the mutual regulation that the GATA factors impose on each other (7) as well as to the different sensitivities of NCR transcription factors to the repressing nitrogen source.

Besides the impact on nitrogen metabolism, the presence of different nitrogen sources also affects the carbon metabolism, e.g., via the TCA cycle intermediate α-ketoglutarate, which serves as a precursor for the synthesis of L-glutamate and as an amino donor for the synthesis of other amino acids, amino sugars, and nucleotides. α-Ketoglutarate is aminated by the

* Corresponding author. Mailing address: Center for Microbial Biotechnology, BioCentrum-DTU, Technical University of Denmark, Building 223, DK-2800 Kgs. Lyngby, Denmark. Phone: (45) 45252696. Fax: (45) 45884148. E-mail: jn@biocentrum.dtu.dk.

† Supplemental material for this article may be found at http://aem.asm.org/.

TABLE 1. Physiological parameters of strain CEN.PK113-7D when cultivated in nitrogen-limited chemostats[a]

| Nitrogen source | Yield | | | Residual glucose (g/liter) | Biomass (g/liter) | $r_{succ}$[e] | $r_{CO_2}$[f] | Carbon balance (%) |
|---|---|---|---|---|---|---|---|---|
| | $Y_{Gx}$[b] | $Y_{Nx}$[c] | $Y_{Ge}$[d] | | | | | |
| $NH_4^+$ | 0.22 ± 0.01 | 1.18 ± 0.04 | 0.26 ± 0.01 | 0.59 ± 0.12 | 1.45 ± 0.05 | 0.02 ± 0.00 | 10.0 ± 0.9 | 100 ± 1 |
| Gln | 0.21 ± 0.01 | 1.38 ± 0.07 | 0.29 ± 0.01 | 1.15 ± 0.14 | 1.36 ± 0.11 | 0.07 ± 0.04 | 12.8 ± 1.1 | 100 ± 4 |
| Ala | 0.20 ± 0.01 | 1.41 ± 0.09 | 0.32 ± 0.03 | 0.92 ± 0.05 | 1.33 ± 0.07 | 0.08 ± 0.01 | 12.5 ± 1.0 | 97 ± 4 |

[a] Each data point represents the average and standard deviation of three separate chemostat steady states.
[b] $Y_{Gx}$, yield coefficient of biomass (g/g of glucose consumed).
[c] $Y_{Nx}$, yield coefficient of biomass (g/nitrogen mmol of respective nitrogen source consumed).
[d] $Y_{Ge}$, yield coefficient of ethanol (g/g of glucose consumed).
[e] $r_{succ}$, mmol of succinate produced/g of biomass/h.
[f] $r_{CO_2}$, mmol of $CO_2$ produced/g of biomass/h.

glutamate dehydrogenases Gdh1 and Gdh3 and by the glutamate synthase-glutamine synthase pathway encoded by *GLT1* and *GLN1* (2). The fluxes through the α-ketoglutarate node are therefore highly dependent on the nitrogen source, as in the case of ammonium, which will lead to a higher net use of α-ketoglutarate than will amino acids such as L-glutamine. The retrograde synthesis of α-ketoglutarate from oxaloacetate is regulated at the transcript level by Rtg2, which represses a repressor, Mks1, resulting in activation of the transcription factors Rtg1 and Rtg3 (26). A recent study shows that the intracellular ammonium concentration induces the activity of Rtg2 and thereby the net production of α-ketoglutarate (44).

However, it is still unclear how nitrogen and carbon metabolism is affected when cells are grown on amino acids such as L-alanine, where the carbon backbone feeds into the TCA cycle via acetyl coenzyme A (acetyl-CoA). The close links between the carbon and nitrogen biochemistry, at the metabolic level as well as the regulatory level, therefore makes it important to understand how cells will respond to growth on different nitrogen sources.

We have consequently examined the impact of ammonium, L-alanine, and L-glutamine on the physiology and transcriptome of the yeast *S. cerevisiae*. Ammonia and L-glutamine enter metabolism via the glutamine and glutamate dehydrogenases and are classified as preferable nitrogen sources that induce NCR (29). L-Alanine, on the other hand, enters metabolism via acetyl-CoA, and its impact on regulation is largely unknown. Cells were grown in well-controlled aerobic chemostat cultures at a growth rate μ of 0.2 $h^{-1}$ with ammonia, L-glutamine, L-alanine, or glucose as the limiting nutrient. Chemostat cultivation allowed the identification of nitrogen source responses at constant nutrient levels and constant growth rates and thereby minimized the number of confounding parameters found in batch cultivations (12). Finally, we linked the physiological data to the transcriptome data by the use of an enzyme subnetwork analysis combined with cluster and promoter analysis.

## MATERIALS AND METHODS

**Strain and maintenance.** This study was performed with the prototrophic haploid laboratory strain *S. cerevisiae* CEN.PK113-7D (*MAT*α) (46), which was provided by P. Kötter from the EUROSCARF strain collection (Frankfurt am Main, Germany). A frozen stock culture was used for the preculture, which was grown in a two-baffle shake flask (500 ml) containing 100 ml of minimal medium (48) at 30°C for 24 h in an orbital shaker at 150 rpm and a pH of 6.5.

**Chemostat cultivation.** Steady-state aerobic chemostat cultures were grown at 30°C by use of 2-liter bioreactors (Applikon) with a working volume of 1.0 liter at a dilution rate *D* of 0.2 (± 0.005) $h^{-1}$. Cultures were fed with a modified minimal medium containing a nitrogen source at a concentration corresponding to 6 mM nitrogen and 250 mM glucose (calculated on nitrogen and carbon atom bases, respectively), which ensured that growth was limited by the nitrogen source and that glucose was in excess. Three different nitrogen sources were used in the three comparative experiments: ammonium sulfate $(NH_4)_2SO_4$, L-glutamine, and L-alanine. All other substrates were in excess. The pH was measured online and kept constant at 5.0 by automatic titration with 4 M KOH by use of an Applikon (ADI1030) biocontroller. The stirring speed was set to 700 rpm, and the dry airflow rate was 1.0 liter/min. The exhaust gas from chemostat cultivation was led through a condenser, and the mole-% values for carbon dioxide and oxygen were measured online by use of a personal computer-controlled acoustic gas analyzer (Brüel & Kjær, Denmark). After batch cultivation, dry weight, metabolite concentrations, and gas profiles were monitored, and when they were constant over at least five residence times, steady state was assumed. Thereafter, samples for RNA extraction were taken. All samples were collected by no later than 10 to 15 residence times from the start of continuous operation to avoid any strain adaptation generally occurring over long-term cultivation (15).

**Media.** The nitrogen-limited minimal medium composition was based on that described in the work of Klein et al. (24). The amounts per liter of the compounds were as follows: $KH_2PO_4$, 3 g; $MgSO_4 \cdot 7H_2O$, 0.5 g; D-glucose, 7.5 g; antifoam 289 (A-5551, Sigma-Aldrich), 0.05 ml; EDTA (Titriplex III), 15.0 mg; $ZnSO_4 \cdot 7H_2O$, 4.5 mg; $MnCl_2 \cdot 2H_2O$, 0.82 mg; $CoCl_2 \cdot 6H_2O$, 0.3 mg; $CuSO_4 \cdot 5H_2O$, 0.3 mg; $Na_2MoO_4 \cdot 2H_2O$, 0.4 mg; $CaCl_2 \cdot 2H_2O$, 4.5 mg; $FeSO_4 \cdot 7H_2O$, 3.0 mg; $H_3BO_3$, 1.0 mg; KI, 0.1 mg; biotin, 0.05 mg; *p*-benzoic acid, 0.2 mg; nicotinic acid, 1.0 mg; Ca-pantothenate, 1.0 mg; pyridoxin-HCl, 1.0 mg; thiamine-HCl, 1.0 mg; and *m*-inositol, 25.0 mg. The nitrogen source in the medium was 6 nitrogen mmol per liter for all the nitrogen-limited chemostat experiments. This corresponded to the following: $(NH_4)_2SO_4$, 0.4 g/liter; L-glutamine, 0.4425 g/liter; or L-alanine, 0.534 g/liter. Media for three glucose-limited chemostat cultures had the same composition as those described above, except that the nitrogen concentration was increased to 5.0 g $(NH_4)_2SO_4$ per liter.

**Metabolite and dry-weight analysis.** Culture supernatants were obtained after centrifugation of samples or by immediate filtering through 0.45-μm-pore-size acetate filters (CAMEO 25GAS 0.45; Osmonics) and stored at −20°C. The samples were used for analysis of the residual substrate concentration and extracellular metabolite concentrations. Glucose, ethanol, acetate, glycerol, pyruvate, and succinate were analyzed by high-performance liquid chromatography (HPLC) using an Aminex HPX-87H column (Bio-Rad) (50). Ammonium, L-glutamine, and L-alanine concentrations were analyzed by ion exchange HPLC using a Waters 474 scanning fluorescence detector (3, 46). The same analysis was performed on the feed medium samples. Culture dry weight was determined via filtration and drying (14).

**Transcript analysis.** Samples for RNA isolation were taken from the chemostat cultivations by rapidly sampling 20 ml of culture into a tube with 20 to 30 ml of crushed ice. Thereby, the temperature was lowered to below 4°C in less than 10 s. Cells were quickly pelleted (4,500 rpm at 0°C for 2 min), instantly frozen in liquid nitrogen, and thereafter stored at −80°C. Total RNA was extracted by using a FastRNA kit, Red (BIO 101, Inc., Vista, CA), after the samples were thawed on ice. mRNA extraction, cDNA synthesis, cRNA synthesis, and labeling were performed as described in the Affymetrix GeneChip expression analysis manual. Ten micrograms of cRNA was thereafter hybridized to the oligonucleotide array YG_S98 (Affymetrix, CA) as described in the Affymetrix GeneChip expression analysis manual. The result for each growth condition was derived from three independent chemostat experiments followed by transcript analysis.

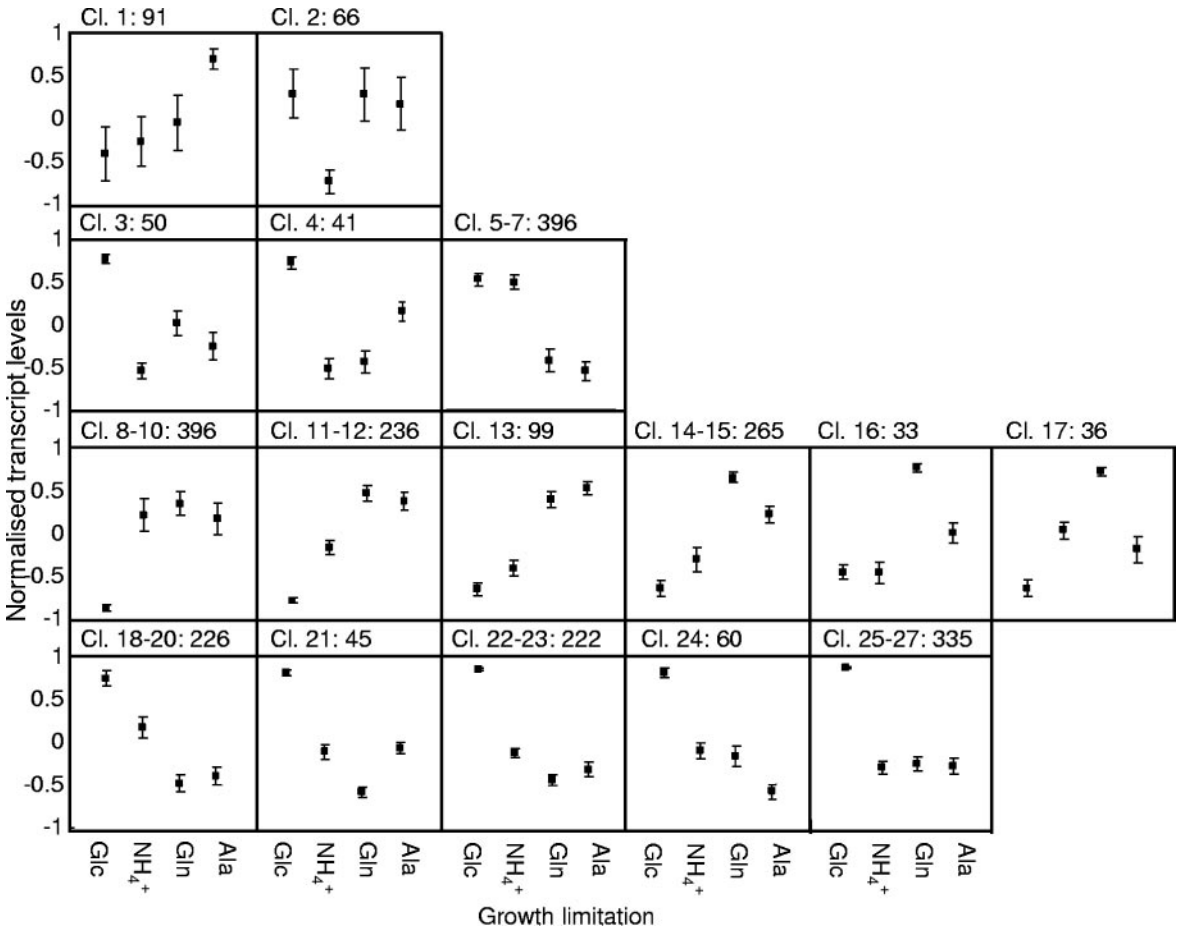


FIG. 1. The transcript profiles of 2,644 genes with altered transcript profiles under glucose, ammonium, L-glutamine, or L-alanine limitation. Genes with similar transcript profiles were divided into 27 solid clusters according to the consensus-clustering algorithm described in reference 35. The transcript level for each transcript is normalized to a value between −1 and 1, where 0 indicates the average expression level over all four conditions. The average transcript level for all genes in a cluster is shown with a black square, while the standard deviation is shown with a bar and the number of genes is shown above the cluster.

**Data acquisition.** The YG_S98 arrays were scanned with the GeneArray scanner, and the Affymetrix microarray suite v5.0 was used to generate CEL image files of the arrays. The array images were then normalized with the software dChip v1.2, and the transcript levels of all 9,335 probe sets were calculated with the perfect-match model in dChip v1.2 (25). The transcript levels of 6,091 unique open reading frames (ORFs) (ORFs defined by the *Saccharomyces* Genome Database) were extracted from the probe sets and used for further analysis.

**ArrayExpress accession number.** The ArrayExpress accession number is E-MEXP-724.

**Data analysis.** Pairwise significance analysis of microarrays (SAM) data analysis of all possible combinations of the four nutrient limitations was performed using the Microsoft Excel SAM add-in (v1.12) (45). Genes with a score greater than a threshold resulting in a false discovery rate of 1% were deemed potentially significant (45).

Cluster analysis was performed on the 2,466 transcripts that were found to alter transcript level under at least one of the four growth conditions (analysis of variance [ANOVA] on the original 6,091 transcripts, 5% significance level). The transcript profiles were clustered into groups of transcripts with similar profiles by use of the software ClusterLustre (19) (see the supplemental material and http://www2.cmb.dtu.dk/additional_material_for_publications/papers/6/index.html). Briefly, the Pearson's correlation coefficient was used as the metric, and the data set was clustered according to the formula $k \cdot r = 20 \cdot 26 = 520$ times; that is, $k = 5 \ldots 30$ clusters and 20 repetitions ($r$) for each cluster size ($k$), with the variational Bayes mixture of Gaussians. The likelihood of the Gaussian mixtures was used to estimate the number of clusters as 27. Clustering with Gaussian mixtures lead to different cluster solutions in each run, and therefore a consensus cluster solution was extracted from the most robust pattern in the initial 520 cluster runs. The 27 clusters were sorted and displayed in a dendrogram, and hence the similarities and differences between the different clusters could be studied. For instance, cluster 1 is more similar to cluster 2 than it is to cluster 3, etc.

Gene expression changes in response to nitrogen limitation were mapped on the genome-scale metabolic model of *S. cerevisiae* (17) in order to identify metabolic hot spots that significantly responded to the nitrogen limitation at the transcriptional level (35). The genome-scale model of yeast was first represented as a graph in which each metabolite is connected to all enzymes that catalyze a reaction involving that particular metabolite. Each enzyme involved in this graph was then scored based on the significance of the change in the expression level of the corresponding gene. This significance score was calculated by using a $t$ test and transforming the resulting $P$ value to a Z-score using the inverse normal cumulative distribution function. Each metabolite was assigned the average score of its $k$ neighboring enzymes, and this score was then corrected for the background by subtracting the mean and dividing by the standard deviation of average scores of 10,000 enzyme groups of size $k$ selected from the same data set. These corrected scores were then converted back to $P$ values by using the normal cumulative distribution function. The 10 top-scoring metabolites were identified as reporter metabolites and selected for further analysis. Thus, the reporter metabolites are those around which transcriptional changes are significantly concentrated.

To uncover the global coordinated response of the genes spread across different metabolic pathways, the genome-scale model was converted to a graph of

enzyme interactions. In this graph, only enzymes are represented as the nodes, and two enzymes sharing a common substrate in the corresponding reactions are connected to each other. Each enzyme in this graph was scored based on its altered transcription level as in the case of reporter metabolite identification. Subnetworks, defined as connected subgraphs of the enzyme interaction graph that showed maximum transcriptional response (quantified as the average background-corrected scores of all enzymes in that subnetwork), were then identified by using a simulated annealing algorithm (see the supplemental material or http://www2.cmb.dtu.dk/additional_material_for_publications/papers/6/index.html).

Promoter analyses were performed using the web-based software Regulatory Sequence Analysis Tools with default settings (http://rsat.ulb.ac.be/rsat/) (47). Promoters (from −800 bp to −1 bp) from genes in each cluster were analyzed for overrepresented hexanucleotides. Hexanucleotides sharing large common patterns were merged by alignment of elements with common patterns. Finally, the relative abundance of the consensus elements was determined by a query against genes in the relevant cluster and a query against genes in the entire genome (5,862 ORFs). Overrepresented gene ontology groups were defined with the Gene Ontology Term Finder (http://db.yeastgenome.org/cgi-bin/GO/goTermFinder) for the *Saccharomyces* Genome Database.

## RESULTS

**Physiological data.** To compare the physiological impacts of different nitrogen limitations, the prototropic *S. cerevisiae* strain CEN.PK113-7D was grown in a chemostat with ammonium, L-glutamine, or L-alanine as a sole and limiting nitrogen source. Chemostat experiments with the three different limitations were performed in triplicate, and HPLC analysis confirmed that the nitrogen source was limiting for growth in all the continuous cultures. The residual concentrations of L-alanine and L-glutamine were found to be below the detection level (<30 μM) in the cultures where they served as nitrogen sources. For the ammonia-limited chemostat, the residual ammonium concentration was found to be 50 μM, which is lower than the $K_m$ of the high-affinity ammonium permease Mep2 (42). The carbon source (glucose) was found to be in excess in all the chemostats (Table 1).

Cells grown under amino acid limitations had biomass yields 17% and 19% higher per nitrogen mole than cells grown under ammonia limitation (Table 1). This indicated a more efficient use of the nitrogen source when cells were grown on amino acids and thereby a change in the nitrogen metabolism between ammonium- and amino acid-limited cultures. The excretion of by-products from the central carbon metabolism was also affected by the nitrogen source. More ethanol, succinate, and $CO_2$ were produced by the amino acid-grown cells than by the ammonium-grown cells, while less glucose was consumed by the amino acid-grown cells (Table 1).

**Consensus cluster analysis.** Aiming to gain insight into the events leading to the physiological changes, we next conducted a whole-genome transcript analysis of the nine nitrogen-limited cultures. To relate these results to conditions where nitrogen was in excess, we also included results from three glucose-limited cultures ($\mu = 0.2\ h^{-1}$) where ammonium was in surplus.

An initial ANOVA of the transcript analysis revealed that 2,644 genes had altered transcript levels in at least one of the four conditions ($P < 0.05$) (see the supplemental material or http://www2.cmb.dtu.dk/additional_material_for_publications/papers/6/index.html). The cluster analysis revealed that the different nitrogen limitations affected as many transcripts (approximately 1,700; clusters 1 to 7, 11 to 21, and 24 [Fig. 1]) as the change to a nitrogen surplus (approximately 1,900; clusters 3 to 12 and 17 to 27 [Fig. 1]). The largest differences between the nitrogen-limited cultures were found between amino acid limitation and ammonium limitation. In 14 of the clusters (clusters 2, 5 to 7, and 11 to 20) (Fig. 1), a total of 1,404 genes had expression profiles under amino acid limitations different from those of cells grown under ammonium limitation.

TABLE 2. Overrepresented sequences retrieved from the promoters of coregulated genes

| Regulatory cluster(s) | Promoter element coverage[a] | Cluster coverage (%) | Genome coverage (%) | Putative binding protein(s)[b] |
|---|---|---|---|---|
| 1 | **GATAAG** | 49 | 32 | Gln3, Gat1, Dal80, Gzf3 |
| 2 | NS | | | |
| 3 | NS | | | |
| 4 | NS | | | |
| 5–7 | NS | | | |
| 8–10 | AA**GATAAG** | 45 | 32 | Gln3, Gat1, Dal80, Gzf3 |
| 11–12 | NS | | | |
| 13 | **TAAACA** | 68 | 53 | Fkh1? |
| 14–15 | **GAAAAAG** | 49 | 40 | |
| 16 | NS | | | |
| 17 | NS | | | |
| 18–20 | NS | | | |
| 21 | NS | | | |
| 22–23 | **AATCAT** | 58 | 47 | ? |
| 24 | NS | | | |
| 25–27 | **TACCCCA** | 27 | 18 | Mig1 |
| | **CCNNYNRNCCG**[c] | 15 | 8 | Cat8 |
| | **WGCCGCCGA**[c] | 4 | 2 | Ume6 |

[a] Sequences shown in bold were searched in promoters of a given cluster or in all genes in the genome. NS, no significant motif detected.

[b] Putative binding proteins were identified using the supplementary material to reference 18. A question mark indicates unavailable or low-confidence information.

[c] Redundant nucleotides are indicated as follows: W = A or T; Y = C or T; R = A or G; and N = A, C, T, or G.

The most significant feature of transcripts with higher levels under amino acid limitation (Fig. 1, clusters 2 and 11 to 17) was the number of genes involved in chronological aging, cytoskeleton organization (65 transcripts), morphogenesis (39 transcripts), and regulation of the physiology (104 transcripts [20%]). These last-mentioned transcripts were particularly involved in the regulation of the M phase of the mitotic cell cycle, which includes chromosome segregation and cytoskeleton organization. Another fraction consisted of transcripts encoding specific transcription factors (56 transcripts), including *MSN2*, *MSN4*, *MIG2*, and *GCR1*, which are involved in the transcriptional induction of the TCA cycle and glycolytic genes (39), as well as *GLN3*, which encodes one of the two positive GATA transcription factors (7). Though increased levels of transcription factor mRNAs could potentially impose transcriptional effects on other genes, GATA factor targets or Msn2/Msn4 targets were not found to be enriched in these clusters. This observation was also supported by promoter analysis, which showed no overrepresentation of the NCR upstream activating sequence GATAAG or the Msn2/Msn4 upstream activating sequence AGGGG (Table 2).

Furthermore, several hundred genes were found to have lower transcript levels under amino acid limitation (clusters 5 to 7 and 18 to 20). This group was characterized by a weak overrepresentation of 4 genes involved in protein peroxisome

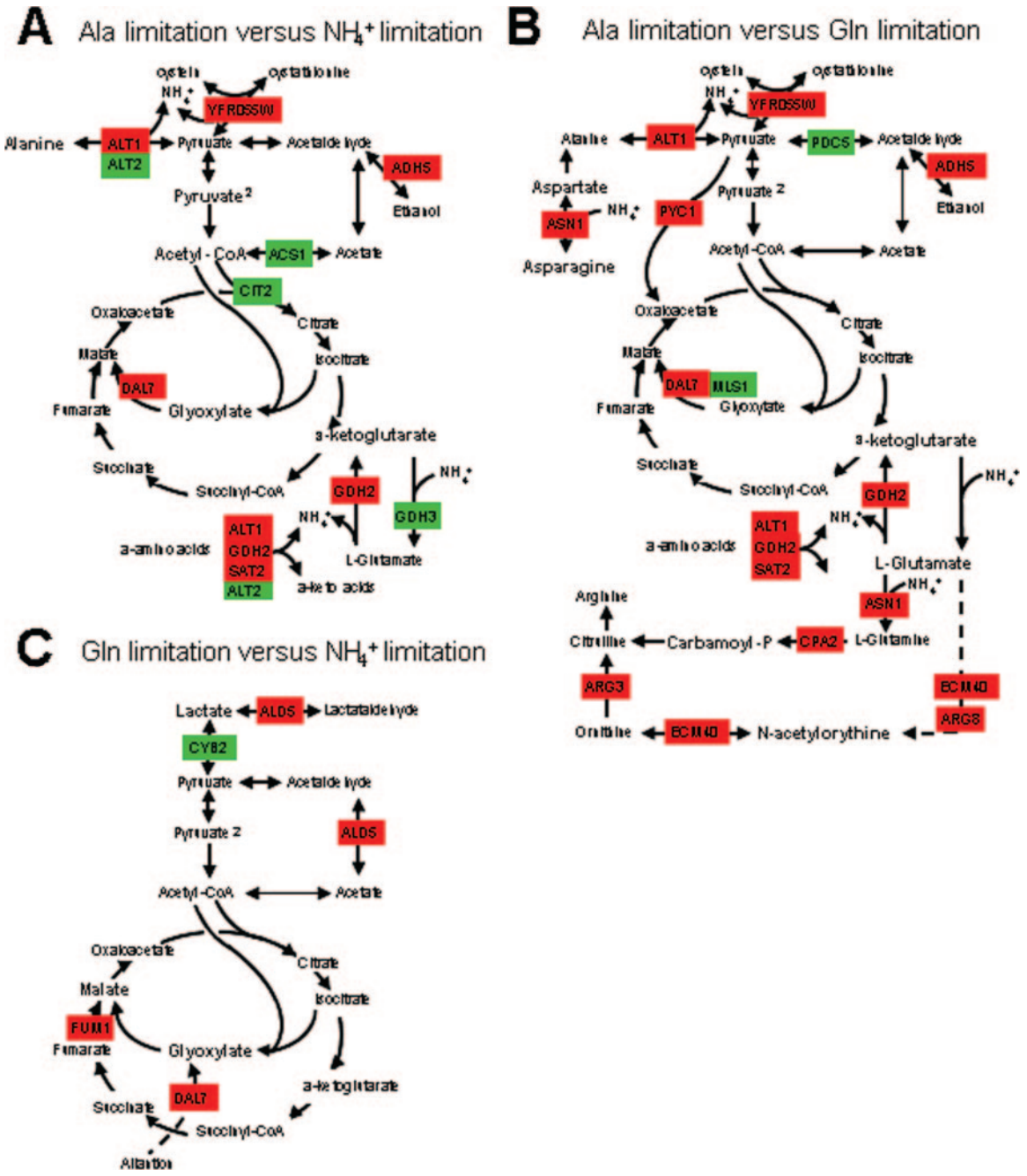


FIG. 2. Yeast metabolic subnetworks affected by ammonium-, L-glutamine-, or L-alanine-limited growth conditions. Reporter metabolites and enzymes were identified by comparing transcript levels of 6,091 unique ORFs from L-alanine-limited cells versus ammonium-limited cells (A), L-alanine-limited cells versus L-glutamine-limited cells (B), and L-glutamine-limited cells versus ammonium-limited cells (C). Reporter metabolites are marked in boldface. (A) Enzymes encoded by genes with transcript levels that are higher under L-alanine-limiting conditions than under ammonium-limiting conditions are shown in red, while enzymes encoded by genes with lower transcript levels under L-alanine-limiting conditions are shown in green. (B and C) A color code identical to that described for panel A is used for the comparison of gene products from L-alanine- versus L-glutamine-limiting conditions (B) and L-glutamine- versus ammonium-limiting conditions (C). Solid lines represent a single reaction, while dashed lines represented several reactions between two metabolites. The three schemes are based on the reporter metabolites (Table 3), the genes encoding enzymatic subnetworks (Table 4), and the corresponding transcriptional changes (see the supplemental material or http://www2.cmb.dtu.dk/additional_material_for_publications/papers/6/index.html).

targeting, of 25 in structural components of ribosomes, and of 38 involved in intracellular transport. These biological functions could all be important for a more efficient nitrogen utilization of cells grown on amino acids (Table 1).

Hence, the consensus cluster analysis together with promoter and gene ontology analysis revealed a large and complex transcript response to amino acid limitation but gave little information about the link to the physiological data (Table 1).

TABLE 3. Reporter metabolites identified in comparisons of two nitrogen limitations[a]

| Gln vs $NH_4^+$ | | | Ala vs $NH_4^+$ | | | Ala vs Gln | | |
|---|---|---|---|---|---|---|---|---|
| Metabolite | No. of genes | *P* value | Metabolite | No. of genes | *P* value | Metabolite | No. of genes | *P* value |
| (*S*)-Lactate[b] | 2 | 6.9E−04 | Allantoin | 2 | 1.1E−04 | L-Glutamate | 41 | 4.8E−04 |
| Phosphatidylethanolamine | 2 | 6.2E−03 | Pyruvate[b] | 6 | 6.9E−04 | α-Ketoglutarate | 20 | 9.7E−04 |
| Malate | 8 | 8.2E−03 | 3-Carboxy-4-methyl-2-oxopentanoate | 2 | 1.3E−03 | Pyruvate | 13 | 2.6E−03 |
| Intermediate methylzymosterol I | 2 | 8.2E−03 | α-Ketoglutarate | 20 | 4.7E−03 | L-Asparagine | 8 | 3.5E−03 |
| Intermediate zymosterol I | 2 | 8.2E−03 | (*R*)-2-Oxoisovalerate | 2 | 6.2E−03 | Carbamoyl phosphate | 3 | 4.7E−03 |
| Hydroxymethylbilane | 2 | 8.2E−03 | Acetyl-CoA | 19 | 8.2E−03 | Maltose | 3 | 4.7E−03 |
| Glyoxylate | 6 | 1.1E−02 | Homocysteine | 7 | 1.1E−02 | *N*2-Acetyl-L-ornithine[b] | 2 | 4.7E−03 |
| ITP | 2 | 1.4E−02 | IMP | 11 | 1.1E−02 | L-Aspartate | 14 | 6.2E−03 |
| GTP | 9 | 1.8E−02 | Glyoxylate | 6 | 1.8E−02 | L-Glutamate[b] | 7 | 8.2E−03 |
| FMN | 3 | 2.3E−02 | L-Alanine | 10 | 1.8E−02 | Allantoin | 2 | 8.2E−03 |

[a] "No. of genes" indicates the number of genes with altered transcript levels which encode enzymes involved in the synthesis or degradation of the reporter metabolite. Metabolites were ordered according to the *P* value scored in the genome-scale metabolic model.
[b] Metabolite located in the mitochondrion.

We therefore used a new model-driven approach (35) to get a better understanding of the molecular mechanisms controlling the differential response to ammonium and amino acids.

**Reporter metabolite analysis.** The bioinformatics tool used here is based on the hypothesis that expression of genes encoding enzymes is coordinated in order to satisfy the metabolic demands of the cell. This assumption implies that metabolic changes can be predicted through the transcriptional changes of genes encoding enzymes in the same metabolic pathway. The tool, reporter metabolite analysis, therefore identifies these groups of genes (subnetworks) rather than individual genes. Metabolites serving as substrate or product for the corresponding enzymes are called "reporter metabolites" and are identified as follows.

First, for each pair-wise comparison of studied conditions, the changes in transcript levels of all genes encoding enzymes are determined by using the classical *t* test. Metabolites are then scored based on the average *P* value (calculated from the *t* test) of their *k* neighboring enzymes. Thus, an enzyme contributes towards the scores of all metabolites that participate in the corresponding reactions. In order to test the statistical significance of the metabolite scores, we corrected the individual metabolite scores by using the mean and the standard deviations of the average scores of 10,000 randomly selected enzyme groups of size *k*. These corrected scores were then converted to *P* values by using the normal cumulative distribution. A high score is consequently equivalent to a low *P* value. The 10 metabolites with the lowest *P* values were identified as reporters. In order to explore a very large proportion of all known enzymes and metabolites from *S. cerevisiae*, we used a genome-scale metabolic model (17) with 1,175 reactions (708 gene products) and 584 metabolites.

The reporter metabolites indicate specific parts of metabolism where significant transcriptional regulation is exerted either to maintain homeostasis or to adjust the metabolite levels to altered demands or both. Similarly, enzyme subnetworks denote which groups of enzymes are functionally connected through metabolic networks and also respond significantly at the transcription level. These subnetworks usually span several metabolic pathways and thus offer a global view of the transcriptional response in a metabolic network (see the supplemental material or http://www2.cmb.dtu.dk/additional_material_for_publications/papers/6/index.html). The subnetworks, together with the reporter metabolites, thereby projected potential metabolic changes and hot spots in response to different nitrogen sources (Fig. 2 and Tables 3 and 4).

Reporter metabolite analysis of the ammonium- versus L-glutamine- and L-alanine-limited cultures suggested that the main changes occur around the TCA cycle and the glyoxylate

TABLE 4. Genes[a] encoding enzymes that synthesize the reporter metabolites listed in Table 3

| Gln vs $NH_4^+$ | Ala vs $NH_4^+$ | Ala vs Gln |
|---|---|---|
| *ADK1* | *ACS1* | *ADH5* |
| *ALD5* | *ADH5* | *ARG3* |
| *AMD2* | *ARG8* | *ARG8* |
| *CKI1* | *ARO8* | *ARO4* |
| *COQ2* | *BAT2* | *ASN1* |
| *CYB2* | *CIT2* | *BAT2* |
| *DAL3* | *COQ2* | *CPA2* |
| *DIC1* | *DAL7* | *DAL7* |
| *ERG25* | *ERG1* | *ECM40* |
| *ERG26* | *FUN63* | *FAA1* |
| *FMN1* | *GDH2* | *FOX2* |
| *FOL1* | *GDH3* | *FSP2* |
| *FOX2* | *MAL31* | *FUN63* |
| *FUM1* | *ODC2* | *GDH2* |
| *FUR4* | *PUR5* | *HIS1* |
| *HEM12* | *SAM3* | *HXK2* |
| *HEM4* | *SAM4* | *KRS1* |
| *HMG2* | *THI6* | *LYS9* |
| *ILV2* | *YDR111C* | *MEP3* |
| *KTR4* | *YFR055W* | *MLS1* |
| *MAL31* | *YLR089C* | *OAC1* |
| *NAT2* | | *ODC2* |
| *PMA1* | | *PDC5* |
| *PSD2* | | *PMI40* |
| *RIB1* | | *PYC1* |
| *RIB5* | | *RHR2* |
| *THI7* | | *SER33* |
| *TRP4* | | *THI6* |
| *TYR1* | | *YDR111C* |
| *YDL100C* | | *YFR055W* |
| *YEL041W* | | *YGR287C* |
| *YLR231C* | | *YLR089C* |

[a] Genes are listed alphabetical order for each comparison. Underlined genes were also identified as significantly changed by ANOVA.


**Cluster 1 (91 gene)**
**UNCLASSIFIED GENES**
*YLR257W NNT1 YLR412W YDR090C AGE1 YHR100C PCI8 YER087C-A YLR108C UTP22 YJL213W YGL196W YFR044C YHL021C YOR203W TMT1 YDR520C ICY1 YBR281C YER068C-A YJL162C YFR016C YDL062W YBR147W YNR068C YDL063C YGR054W*
**amino acid metabolism**
*CPA2 LEU4 ASN1 UGA1 YFR055W CHA1 YLR089C GDH2 BAT2 CPA1 ECM17 HOM3*
**transport routes**
*DAL4 OAC1 VMA7 VID24 SAC1 POR1 SXM1 GEA2 YHM1 SED4 UBC4*
**cell cycle**
*BMH1 CIN1 CBF2 PTP3 CHL4 SCC2 RPG1*
**transported compounds (substrates)**
*MEP3 DAL4 OAC1 DIP5 VMA7 SXM1 YHM1*
**RNA synthesis**
*TFG1 STB5 SAS3 SIR4 YKR064W HAP4*
**nitrogen and sulfur metabolism**
*DCG1 UGA1 YLR089C GDH2 DAL1 ECM17*
**nucleotide metabolism**
*IMD2 DAL7 DAL1 IMD1 SDT1 IMD3*
**C-compound and carbohydrate metabolism**
*PYC1 YGR287C FSP2 DAL7 PDA1*
**cellular sensing and response**
*PTP3 GPR1 SAS3 UBC4 SIR4*


**Cluster 8 (135 genes)**
**UNCLASSIFIED GENES**
*YER188W ADY3 YHR080C YLL029W YHR049C-A YHR202W HRT3 GAS3 EDE1 HSP31 YDR433W HLR1 YGR190C YDR539W YOR022C YIL165C YNL170W YMR252C YPL150W GYP5 RSB1 GPI17 YMR316C-A YMR173W-A YNL311C YDL211C SYP1 RMD8 MSC2 YPL095C NIT1 YGR210C GWT1 CSM2 GID8 PRM7 YMR316C-B YGR035C COS4 YDL146W YNL234W YNR065C YMR247C YHL026C YOR086C YLR460C*
**transport routes**
*YEL006W MUP1 FCY2 FAB1 TFP1 GFD1 NCE103 MYO4 VPH1 STV1 YGL114W ERS1 MSN5 VPS8*
**transported compounds (substrates)**
*TPO2 MUP1 FCY2 TFP1 VPH1 STV1 NHA1 YLL055W TPO4 YMR088C TPN1 KHA1*
**cell cycle**
*CDC55 SPS18 RAP1 MYO4 TEL1 MUM2 SPC110 CDC47 RCK2 NDD1*
**cellular sensing and response**
*MFA1 SAG1 STE5 MYO4 AGA2 MFA2 MSN5 ROM2*
**fungal/microorganismic cell type differentiation**
*CDC55 BUD5 SPS18 PHD1 GSC2 MYO4 MUM2 ROM2*
**amino acid metabolism**
*DUR1,2 MUP1 YIL167W HIS2 YHR112C GLT1 APE2*
**C-compound and carbohydrate metabolism**
*MIG1 RAP1 GSC2 OST6 YPR1 YHR210C ROM2*
**lipid, fatty acid and isoprenoid metabolism**
*FAB1 OPI3 TEL1 YJR107W ACC1 PIS1 ELO1*
**protein targeting, sorting and translocation**
*FAB1 VPH1 ERF2 YCR099C ERS1 VPS8 VPS38*


**Cluster 9 (94 genes)**
**UNCLASSIFIED GENES**
*VAC14 YHR095W YOL107W YBL081W YGR125W YBL029W RMD11 YGK3 YIL089W YLR199C YOR015W FIT1 YJR098C DEM1 YIR007W YDR094W YJR061W YNL129W YCR102C YLR156W YPR130C*
**RNA synthesis**
*RGR1 ASH1 RIM101 RRN7 ZMS1 PTR3 SRB2 HST3 DAL80 PHO85 DBF2 YML081W HIR3*
**transport routes**
*NPR1 SEC26 VTH2 GAP1 PMR1 AVT6 DAL5 YAP1801 HXT1 GAA1 MEP2 VMA4*
**cell cycle**
*RIM101 FAR1 KCC4 CDC48 RAD54 VAN1 PHO85 DBF2 RDH54 RED1 HIR3*
**transported compounds (substrates)**
*DUR3 GAP1 PMR1 AVT6 DAL5 HOL1 HXT1 MEP2 VMA4*
**C-compound and carbohydrate metabolism**
*GPH1 RGR1 MNN1 PYC2 ADH1 PHO85 PIG2*
**DNA processing**
*RSC2 RAD54 MCM3 HPR5 RDH54 RNR1 RED1*
**fungal/microorganismic cell type differentiation**
*RGR1 ASH1 FAR1 HSP150 VAN1 YAP1801 CIS3*
**protein degradation**
*PRB1 CPS1 YBR139W CDC48 ULP1 LAP3 PUP1*
**amino acid metabolism**
*PUT2 AVT7 ASP3-1 HOM6*


**Cluster 10 (167 genes)**
**UNCLASSIFIED GENES**
*YMR010W YGL140C YPR117W YOR154W YLR064W YKR090W YDR326C YEL067C YKR077W CWC25 YHR029C YLR454W YPL158C YNL176C RMD6 YLL032C ZRG8 YOL019W YGL176C FAR11 YBR287W YHL029C YDL237W FSH1 YPL030W YMR155W SUR7 YNL042W YGR106C YNL087W YIR042C YLR177W YHR078W YKR021W*
**transport routes**
*VPS15 PUT4 ITR1 BST1 VPS54 HXT4 NHX1 VMA5 YCF1 SEC24 PET9 MTR10 SEC7 PEP1 NUP145 EXO84 AVT1 SEC31 YIL006W TRS120 CHC1 MUP3 CTR2 NUP157*
**transported compounds (substrates)**
*PUT4 ITR1 YBR235W PMP2 HXT4 SGE1 NHX1 VMA5 PET9 MTR10 NUP145 AVT1 YIL006W PHO91 PMA1 YPR003C DNF1 MUP3 CTR2*
**cell cycle**
*YCG1 SIS2 NAM8 ARD1 SPC97 BEM2 SMC1 CDC15 VHS2 FAR11 NUD1 TOR1 CLN3 CLA4 ECM38 TOM1*
**RNA synthesis**
*TFC4 TRA1 CHA4 SIS2 CTK3 GCN4 GAL80 GZF3 ASK10 IXR1 STD1 STB6 GAL83 HST1 GAT1*
**amino acid metabolism**
*PUT1 YKL218C CHA4 HIS4 GCN4 LEU1 HIS7 TRM5 SDL1 ECM38 MUP3 ADE3 SAM2*
**fungal/microorganismic cell type differentiation**
*EXG2 KEL1 AMA1 BEM2 YGR221C AXL1 CLN3 SBE22 CLA4 EXO84 TRM5 MSB2 GIC2*
**transport facilitation**
*PMP2 YOL163W YIL056W VMA5 YCF1 NEW1 YHL035C OPT2 YIL006W PMA1 DNF1*
**C-compound and carbohydrate metabolism**
*EXG2 PMT1 GAL80 YMR237W OST3 STD1 DIE2 PMT4 GAL83*


**Cluster 11 (114 genes)**
**UNCLASSIFIED GENES**
*YML020W YDR352W YDR089W FUN21 YDR540C DOP1 YBR007C YBP1 MON2 YPL137C YIL060W IST2 TCO89 CYK3 YPR097W YMR266W RIM20 YOL036W YML072C YGR102C YJL028W YKR089C YPL184C*
**transport routes**
*GEF1 KIP1 MRS4 TOK1 PTR2 VRP1 FUR4 GLE1 VMA13 GGA2 SLA1 AVT4 KAP123 KIP2 GEA1 LYP1 MYO2 CUP5*
**cell cycle**
*BCK1 KAR9 KIP1 TOR2 ULP2 PRP8 DDC1 NUM1 KIP2 MLH1 TUB1 SCH9 ACE2 SPT16*
**RNA synthesis**
*SIN3 ORC1 MOT1 CYC8 SWI5 RGT1 TUP1 TEA1 MED1 CHD1 SCS2 TAO3 ACE2*
**fungal/microorganismic cell type differentiation**
*BCK1 BOI2 SIN3 VRP1 SLA1 BUD8 BEM3 MYO2 MNN10 BUD4 RVS167 CHS3*
**C-compound and carbohydrate metabolism**
*TPS3 PDC1 RGT1 ENO2 PFK1 MNN10 SCS2 ACE2 CHS3*
**cell growth / morphogenesis**
*BCK1 BOI2 TOR2 VRP1 SLA1 BUD8 BEM3 SCH9 RVS167*
**transported compounds (substrates)**
*GEF1 FUR4 GLE1 VMA13 AVT4 LYP1 TPO1 YBT1 CUP5*


**Cluster 12 (122 genes)**
**UNCLASSIFIED GENES**
*CAF120 YMR221C YNL321W YGL204C YLR455W YER140W YPL014W PIN4 SCY1 YGR068C YEL043W YML018C YGR069W YBR113W YNR014W YPL066W AVO1 YCR026C PSK2 YDL073W CYM1 YIL151C YHR151C*
**fungal/microorganismic cell type differentiation**
*HOC1 CHS2 PMD1 RIM13 MYO5 BNI1 ZDS1 MSB1 PAM1 LAS17 GIC1 LRG1 MYO1 DOA4 GRR1 ECM33 SVL3 STE20 SET1*
**RNA synthesis**
*SWI1 HAC1 CDC13 RSC6 RPO21 STB3 YLR278C STH1 MSN4 DOT6 SPT15 MIG2 HCM1 SPP41 YPR115W MOT2 INO80 RCS1 RPA190*
**cell cycle**
*CDC13 RSC6 ESP1 BUB1 STH1 BNI1 ZDS1 LAS17 KIP3 CLB6 CIN8 MYO1 GRR1 KIC1 ECM33 SET1*
**transport routes**
*STE6 SEC16 MYO5 SEC8 BPH1 FET5 KIP3 CIN8 KAP122 MYO1 GRR1 VMA2 SCD6 HNM1*
**cell growth / morphogenesis**
*VTC1 HOC1 BNI1 MNN2 ZDS1 MSB1 PAM1 LAS17 GIC1 MYO1 GRR1 SVL3 STE20*
**C-compound and carbohydrate metabolism**
*HOC1 SWI1 CHS2 YNL201C PFK2 MSN4 CDC19 PFK27 STT3 MIG2 GRR1*

cycle (Fig. 2A and C). This was especially the case for L-alanine versus ammonium, where pyruvate, acetyl-CoA, glyoxylate, and α-ketoglutarate were identified as reporter metabolites (Fig. 2A and Table 3). The flux from L-alanine to acetyl-CoA was potentially increased by the upregulation of the putative L-alanine-transaminase gene *ALT1* (Fig. 2A). Acetyl-CoA and glyoxylate could further be converted into malate via an increased level of the malate synthase, Dal7. The main function of the malate synthase is to increase anabolic activity and to make possible the synthesis of four and six carbons from the two-carbon level of acetyl-CoA.

A similar effect was found for the L-glutamine-limited cells compared to cells grown under ammonium limitation. Here, the glyoxylate cycle intermediates glyoxylate and malate were identified as reporter metabolites when L-glutamine served as the nitrogen source (Fig. 2C). The latter analysis also suggested that changes in the nitrogen source influenced the metabolism of complex lipids, since intermediates in ergosterol biosynthesis (methylzymosterol and zymosterol) and in phospholipid metabolism (phosphatidylethanolamine) were identified as reporter metabolites (Table 3).

The model-driven data analysis also revealed large changes between the L-alanine-limited and the L-glutamine-limited growth conditions. In this case, the reporter metabolites suggested changes primarily in amino acid metabolism (Fig. 2B), with little effect on the glyoxylate cycle. Most of the genes with higher transcript levels in the L-alanine-grown cells, as identified by enzyme subnetwork analysis, were involved in transaminase and deaminase reactions, a pattern that suggests a higher ammonium turnover in the L-alanine-grown cells. The reporter genes were primarily found in cluster 1 from the clustering analysis (*ALT1*, *ASN1*, *BAT2*, *CPA2*, *DAL7*, *GDH2*, *PYC1*, and *YFR055W*) (Fig. 3) where transcript levels were higher on L-alanine than on L-glutamine or ammonium.

**Promoter analysis.** All in all, three clusters (1, 4, and 24 [Fig. 1]) identified 192 genes with changed transcript levels for L-alanine-grown cells. Cluster 1 had an overrepresentation of genes (49%) with the GATAAG NCR *cis*-acting element (Table 2), indicating that ammonium and L-glutamine could impose NCR, despite the low levels of these compounds in the medium. This result would also explain a majority of the changes in the reporter metabolite analysis between L-alanine-limited and L-glutamine-limited cells (Fig. 2A). Genes in this cluster (91 genes) were involved in nitrogen and amino acid metabolism (*ALT1*, *ASN1*, *BAT2*, *CHA1*, *CPA1*, *CPA2*, *DAL1*, *DCG1*, *ECM17*, *FOL1*, *GDH2*, *HOM3*, *LEU4*, *MCT1*, *PDA1*, *UGA1*, and *YFR055W*), transport (*DAL4*, *DIP5*, *MEP3*, *OAC1*, *SXM1*, *VMA7*, and *YHM1*), and nucleotide metabolism (*DAL7*, *DAL1*, *IMD1*, *IMD2*, *IMD3*, and *SDT1*). Many of these genes have previously been described as targets for NCR.

However, it was surprising to find the classical NCR-sensitive genes in cluster 1, since the shape of this cluster indicated that L-glutamine and ammonium induced repression even though they are limiting for growth. NCR-sensitive genes have previously been found to be repressed in media where ammonium is in excess (7, 44). The current data revealed a second group of NCR-sensitive genes in clusters 8 to 10 (Fig. 1). These clusters represented genes with lower transcript levels in the glucose-limited cultures where ammonium was in excess. The current data therefore indicate that NCR-sensitive genes can be divided into two groups, one that responds to nitrogen in concentrations below 30 μM and another group that responds to nitrogen in the millimolar range.

The promoter analysis also revealed that the Mig1 core consensus element, ACCCC, the Ume6 consensus element, WGCCGCCGA, and the Cat8 consensus element, CCNNYN RNCCG, were overrepresented in clusters 25 to 27. A higher transcript level characterized these clusters when cells were grown under glucose-limiting conditions where glucose was in excess. This observation correlates with previously published results (6), where cells were found to be under Mig1 and Ume6 regulation when grown under nitrogen-limited conditions.

## DISCUSSION

In the current paper, we have shown that cells grown with amino acids as the limiting nitrogen source have altered metabolism with higher biomass yields per nitrogen mole than cells grown under ammonium-limiting conditions. To understand these metabolic changes, we measured the global transcript levels and analyzed the results with two novel expression analysis tools developed in our laboratory (19, 35). The cluster analysis revealed 18 clear clusters of genes that had changed transcript levels in response to one of the nitrogen sources, containing a total of approximately 1,700 transcripts (Fig. 1, clusters 1 to 7 and 11 to 21). Another set of 21 clusters covered genes that had changed expression in response to glucose limitation (approximately 1,900 genes in clusters 3 to 12 and 17 to 27). Whole-genome transcript profiles have previously been compared for *S. cerevisiae* grown in glucose-limited culture and that grown in ammonium-limited culture ($\mu = 0.1\ h^{-1}$) (6, 44). In this case, transcript profiles were sorted with SAM, which led to a total of 301 genes with different transcript levels for the two conditions. These genes were also identified in the current work (76% overlap of clusters 2 to 12 and 21 to 27). As the reader may note, these clusters contained a much larger number of transcripts than the ones identified by the SAM analysis. To investigate if the difference in the number of identified transcripts was due to the choice of analysis tool or the quality of the data in the two data sets, we conducted a similar SAM analysis ($P < 0.01$) with the current data. The SAM analysis identified 560 genes with altered transcript levels. The current consensus cluster analysis combined with ANOVA thus allowed us to extract more information from the transcript data set.

The consensus cluster analysis gave information about the coregulated transcripts (Fig. 1 and 3), while promoter analysis

FIG. 3. Transcript profiles of clusters with NCR-responsive genes. The relative transcript levels of each gene (rows) under the four different growth conditions (columns), where green represents transcript levels between −1 and 0 and red represents transcript levels between 0 and 1, are shown. Genes in each cluster are divided into functional groups that are overrepresented in the given cluster.

of the different gene clusters indicated possible means of regulation (Table 2). However, this analysis provided limited insight into the transcriptional changes causing altered metabolism under the different nitrogen limitations. This shortcoming is primary, due to the equal weight that transcript changes are given in cluster analysis, ignoring the fact that the gene products act in different metabolic pathways and different cellular compartments. One way to include this information is to integrate knowledge about metabolic pathways into the analysis of the transcript data. Such integration enabled us to systematically identify coregulated enzymatic subnetworks as well as the metabolic changes that could follow from a given change.

**Altered anabolic activity in L-alanine-grown cells.** The enzyme subnetwork analysis suggests that L-alanine-grown cells have increased anabolic activity compared to L-glutamine- and ammonium-grown cells via the pyruvate carboxylase gene *PYC1* and the malate synthase gene *DAL7* (Fig. 2A and B), which may explain why L-alanine-grown cells have biomass yields higher than those of ammonium-grown cells. The higher biomass yields may also be supported by increased levels of pyruvate due to higher transcript levels of *YFR055W* and *ALT1* in the L-alanine-grown cells. The enzyme subnetwork analysis also revealed that L-alanine-grown cells could have increased levels of the L-glutamate-degrading L-glutamate dehydrogenase transcript *GDH2* and decreased levels of the citrate synthase transcript *CIT2* (Fig. 2A). Glutamate dehydrogenase and citrate synthase are key enzymes in the fixation of ammonium to amino acids, and altered levels of these enzymes may therefore also contribute to the higher biomass production in L-alanine-grown cells. *CIT2* is induced by the Rtg2/Mks1/Rtg1/3 pathway, which ensures retrograde production of α-ketoglutarate (26), while *GDH2* is repressed by NCR via GATA factors (5). Tate and Cooper have recently suggested a model in which ammonium regulates the level of L-glutamate by induction of *CIT2* via Rtg2 and inhibition of *GDH2* by NCR (44), a hypothesis that is in good agreement with the current enzyme subnetwork analysis (Fig. 2A). Somewhat unexpectedly, both enzyme subnetwork analysis and cluster analysis showed that *GDH2* and other NCR-sensitive genes have lower transcript levels under L-glutamine- and ammonium-limited conditions (Fig. 3, cluster 1), suggesting that concentrations below 50 μM are sufficient to induce NCR. This phenomenon is similar to those observed when cells are exposed to both high and low levels of glucose. In the first case, genes carrying the glucose-repressible Mig1 consensus element have transcript levels in glucose-limited cultures that are higher than those in cultures where glucose is in excess (6) (Fig. 1, clusters 21 to 27). A second group of Mig1-repressible genes appears to be derepressed only when glucose is completely abolished from the media, as observed when glucose-limited cultures are compared to cultures limited for the nonrepressible carbon sources acetate and ethanol (12).

**Changes in the transport properties of nitrogen-limited cells.** This apparent ability to sustain repression at very low L-glutamine and ammonium levels in the media could be due to higher intracellular concentrations. Ammonium uptake and amino acid uptake are driven by the electrochemical gradient across the plasma membrane, and this mechanism can lead to differences between the intracellular concentration and that in the medium of several hundredfold (21, 36). The concentrations of intracellular ammonium and L-glutamine could thereby be held at a repressing level, provided that the corresponding high-affinity transporters are available in the plasma membrane.

The transcript analysis does indeed indicate that cells adapted to nitrogen limitations have changed the uptake of nitrogenous compounds. Previous studies have shown that to maximize the uptake of a limited nitrogen source, the cells have two options: one is to increase the expression of genes encoding high-affinity permeases (30), and the other is to change the transmembrane potential together with a change in the $K_m$ of the transporter (30, 33). The current study shows that the gene encoding the high-affinity ammonium permease, *MEP2*, has higher transcript levels under all three nitrogen limitations than it does under glucose limitation (Fig. 3, cluster 9). This is an observation that supports the first strategy and points to Mep2 being important in the uptake of ammonium under nitrogen-limited conditions (30).

The transcript levels of genes encoding the main L-alanine permeases *GAP1* and *PUT4* were found to be high for all nitrogen limitations (cluster 9), whereas the transcript level of a third L-alanine-permease gene, *DIP5*, was increased only under L-alanine-limiting conditions (cluster 1). This regulation is probably mediated by NCR, as both *GAP1* and *PUT4* are known to be under this regulation (9, 23), while *DIP5* can be repressed by an NCR-inducing nitrogen source (38). Besides the genes encoding specific nitrogen transporters, the plasma membrane $H^+$-ATPase gene, *PMA1*, also had a higher transcript level in the nitrogen-limited cultures (Fig. 3, cluster 10). Pma1 is the main $H^+$-ATPase in the plasma membrane and is essential for the maintenance of the electrochemical gradient across the plasma membrane (41). A potential effect of the higher mRNA is therefore an increase in the membrane potential, suggesting that nitrogen-limited cells also apply the second strategy. According to the Nernst equation for electric potential, this opens the possibility of secondary active transport against a steeper gradient and thereby the uptake of lower concentrations of nitrogen through the nitrogen transporters. Another way to increase the plasma membrane potential is to lower the cytosolic $H^+$ concentration through acidification of the vacuole. A number of transcripts encoding subunits of the vacuolar $H^+$-ATPase (*TFP1*, *STV1*, *VPH1*, *VMA5*, *VMA13*, and *VMA2*) were increased in the nitrogen-limited cultures. However, it is questionable whether the higher transcript levels have a physiological effect, as the $V_1$ domain and the $V_0$ domain of the vacuolar $H^+$-ATPase are known to dissociate and inactivate the ATPase at high glucose concentrations (34).

## ACKNOWLEDGMENTS

This work was supported by grant 26-02-0098 from the Danish Technical Research Councils.

We thank Christoffer Bro for transcriptional data from carbon-limited chemostat cultivations, Lene Christiansen for technical assistance, and Mats Åkesson for assistance with the analysis of the DNA microarray data.

## REFERENCES

1. **Attfield, P. V.** 1997. Stress tolerance: the key to effective strains of industrial baker's yeast. Nat. Biotechnol. **15:**1351–1357.
2. **Avendano, A., A. Deluna, H. Olivera, L. Valenzuela, and A. Gonzalez.** 1997. *GDH3* encodes a glutamate dehydrogenase isozyme, a previously unrecognized route for glutamate biosynthesis in *Saccharomyces cerevisiae*. J. Bacteriol. **179:**5594–5597.

3. **Barkholt, V., and A. L. Jensen.** 1989. Amino acid analysis: determination of cysteine plus half-cystine in proteins after hydrochloric acid hydrolysis with a disulfide compound as additive. Anal. Biochem. **177:**318–322.
4. **Beck, T., and M. N. Hall.** 1999. The TOR signalling pathway controls nuclear localization of nutrient-regulated transcription factors. Nature **402:**689–692.
5. **Blinder, D., and B. Magasanik.** 1995. Recognition of nitrogen-responsive upstream activation sequences of *Saccharomyces cerevisiae* by the product of the *GLN3* gene. J. Bacteriol. **177:**4190–4193.
6. **Boer, V. M., J. H. de Winde, J. T. Pronk, and M. D. Piper.** 2003. The genome-wide transcriptional responses of *Saccharomyces cerevisiae* grown on glucose in aerobic chemostat cultures limited for carbon, nitrogen, phosphorus, or sulfur. J. Biol. Chem. **278:**3265–3274.
7. **Cooper, T. G.** 2002. Transmitting the signal of excess nitrogen in *Saccharomyces cerevisiae* from the Tor proteins to the GATA factors: connecting the dots. FEMS Microbiol. Rev. **26:**223–238.
8. **Coschigano, P. W., S. M. Miller, and B. Magasanik.** 1991. Physiological and genetic analysis of the carbon regulation of the NAD-dependent glutamate dehydrogenase of *Saccharomyces cerevisiae*. Mol. Cell. Biol. **11:**4455–4465.
9. **Courchesne, W. E., and B. Magasanik.** 1983. Ammonia regulation of amino acid permeases in *Saccharomyces cerevisiae*. Mol. Cell. Biol. **3:**672–683.
10. **Crespo, J. L., T. Powers, B. Fowler, and M. N. Hall.** 2002. The TOR-controlled transcription activators GLN3, RTG1, and RTG3 are regulated in response to intracellular levels of glutamine. Proc. Natl. Acad. Sci. USA **99:**6784–6789.
11. **Cunningham, T. S., and T. G. Cooper.** 1993. The *Saccharomyces cerevisiae DAL80* repressor protein binds to multiple copies of GATAA-containing sequences ($URS_{GATA}$). J. Bacteriol. **175:**5851–5861.
12. **Daran-Lapujade, P., M. L. Jansen, J. M. Daran, W. van Gulik, J. H. de Winde, and J. T. Pronk.** 2004. Role of transcriptional regulation in controlling fluxes in central carbon metabolism of *Saccharomyces cerevisiae*. A chemostat culture study. J. Biol. Chem. **279:**9125–9138.
13. **Didion, T., B. Regenberg, M. U. Jorgensen, M. C. Kielland-Brandt, and H. A. Andersen.** 1998. The permease homologue Ssy1p controls the expression of amino acid and peptide transporter genes in *Saccharomyces cerevisiae*. Mol. Microbiol. **27:**643–650.
14. **Dynesen, J., H. P. Smits, L. Olsson, and J. Nielsen.** 1998. Carbon catabolite repression of invertase during batch cultivations of *Saccharomyces cerevisiae*: the role of glucose, fructose, and mannose. Appl. Microbiol. Biotechnol. **50:**579–582.
15. **Ferea, T. L., D. Botstein, P. O. Brown, and R. F. Rosenzweig.** 1999. Systematic changes in gene expression patterns following adaptive evolution in yeast. Proc. Natl. Acad. Sci. USA **96:**9721–9726.
16. **Forsberg, H., and P. O. Ljungdahl.** 2001. Sensors of extracellular nutrients in *Saccharomyces cerevisiae*. Curr. Genet. **40:**91–109.
17. **Forster, J., I. Famili, P. Fu, B. O. Palsson, and J. Nielsen.** 2003. Genome-scale reconstruction of the *Saccharomyces cerevisiae* metabolic network. Genome Res. **13:**244–253.
18. **Gasch, A. P., A. M. Moses, D. Y. Chiang, H. B. Fraser, M. Berardini, and M. B. Eisen.** 2004. Conservation and evolution of cis-regulatory systems in ascomycete fungi. PLoS Biol. **2:**e398.
19. **Grotkjaer, T., O. Winther, B. Regenberg, J. Nielsen, and L. K. Hansen.** 2006. Robust multi-scale clustering of large DNA microarray datasets with the consensus algorithm. Bioinformatics **22:**58–67.
20. **Hinnebusch, A. G.** 2005. Translational regulation of *GCN4* and the general amino acid control of yeast. Annu. Rev. Microbiol. **59:**407–450.
21. **Horak, J.** 1986. Possible role of histidine in the L-proline transport system of *Saccharomyces cerevisiae*. Biochim. Biophys. Acta **862:**407–412.
22. **Iraqui, I., S. Vissers, F. Bernard, J. O. De Craene, E. Boles, A. Urrestarazu, and B. Andre.** 1999. Amino acid signaling in *Saccharomyces cerevisiae*: a permease-like sensor of external amino acids and F-box protein Grr1p are required for transcriptional induction of the *AGP1* gene, which encodes a broad-specificity amino acid permease. Mol. Cell. Biol. **19:**989–1001.
23. **Jauniaux, J. C., and M. Grenson.** 1990. *GAP1*, the general amino acid permease gene of *Saccharomyces cerevisiae*. Nucleotide sequence, protein similarity with the other bakers yeast amino acid permeases, and nitrogen catabolite repression. Eur. J. Biochem. **190:**39–44.
24. **Klein, C. J. L., L. Olsson, and J. Nielsen.** 1998. Nitrogen-limited continuous cultivations as a tool to quantify glucose control in *Saccharomyces cerevisiae*. Enzyme Microb. Technol. **23:**91–100.
25. **Li, C., and W. H. Wong.** 2001. Model-based analysis of oligonucleotide arrays: expression index computation and outlier detection. Proc. Natl. Acad. Sci. USA **98:**31–36.
26. **Liu, Z., and R. A. Butow.** 1999. A transcriptional switch in the expression of yeast tricarboxylic acid cycle genes in response to a reduction or loss of respiratory function. Mol. Cell. Biol. **19:**6720–6728.
27. **Lorenz, M. C., and J. Heitman.** 1998. The MEP2 ammonium permease regulates pseudohyphal differentiation in *Saccharomyces cerevisiae*. EMBO J. **17:**1236–1247.
28. **Magasanik, B.** 1992. Regulation of nitrogen utilization, p. 283–317. *In* E. W. Jones, J. R. Pringle, and J. R. Broach (ed.), The molecular and cellular biology of the yeast *Saccharomyces*. Cold Spring Harbor Laboratory, Cold Spring Harbor, N.Y.
29. **Magasanik, B.** 2005. The transduction of the nitrogen regulation signal in *Saccharomyces cerevisiae*. Proc. Natl. Acad. Sci. USA **102:**16537–16538.
30. **Marini, A. M., S. Soussi-Boudekou, S. Vissers, and B. Andre.** 1997. A family of ammonium transporters in *Saccharomyces cerevisiae*. Mol. Cell. Biol. **17:**4282–4293.
31. **Martin, D. E., A. Soulard, and M. N. Hall.** 2004. TOR regulates ribosomal protein gene expression via PKA and the Forkhead transcription factor FHL1. Cell **119:**969–979.
32. **Mitchell, A. P., and B. Magasanik.** 1984. Three regulatory systems control production of glutamine synthetase in *Saccharomyces cerevisiae*. Mol. Cell. Biol. **4:**2767–2773.
33. **Opekarova, M., T. Caspari, B. Pinson, D. Brethes, and W. Tanner.** 1998. Post-translational fate of CAN1 permease of *Saccharomyces cerevisiae*. Yeast **14:**215–224.
34. **Parra, K. J., and P. M. Kane.** 1998. Reversible association between the $V_1$ and $V_0$ domains of yeast vacuolar $H^+$-ATPase is an unconventional glucose-induced effect. Mol. Cell. Biol. **18:**7064–7074.
35. **Patil, K. R., and J. Nielsen.** 2005. Uncovering transcriptional regulation of metabolism by using metabolic network topology. Proc. Natl. Acad. Sci. USA **102:**2685–2689.
36. **Pena, A., J. P. Pardo, and J. Ramirez.** 1987. Early metabolic effects and mechanism of ammonium transport in yeast. Arch. Biochem. Biophys. **253:**431–438.
37. **Pretorius, I. S.** 2000. Tailoring wine yeast for the new millennium: novel approaches to the ancient art of winemaking. Yeast **16:**675–729.
38. **Regenberg, B., L. During-Olsen, M. C. Kielland-Brandt, and S. Holmberg.** 1999. Substrate specificity and gene expression of the amino-acid permeases in *Saccharomyces cerevisiae*. Curr. Genet. **36:**317–328.
39. **Rolland, F., J. Winderickx, and J. M. Thevelein.** 2002. Glucose-sensing and -signalling mechanisms in yeast. FEMS Yeast Res. **2:**183–201.
40. **Schmitt, A. P., and K. McEntee.** 1996. Msn2p, a zinc finger DNA-binding protein, is the transcriptional activator of the multistress response in *Saccharomyces cerevisiae*. Proc. Natl. Acad. Sci. USA **93:**5777–5782.
41. **Serrano, R., M. C. Kielland-Brandt, and G. R. Fink.** 1986. Yeast plasma membrane ATPase is essential for growth and has homology with (Na+ + K+), K+- and Ca2+-ATPases. Nature **319:**689–693.
42. **Soupene, E., R. M. Ramirez, and S. Kustu.** 2001. Evidence that fungal MEP proteins mediate diffusion of the uncharged species $NH_3$ across the cytoplasmic membrane. Mol. Cell. Biol. **21:**5733–5741.
43. **Stanbrough, M., D. W. Rowen, and B. Magasanik.** 1995. Role of the GATA factors Gln3p and Nil1p of *Saccharomyces cerevisiae* in the expression of nitrogen-regulated genes. Proc. Natl. Acad. Sci. USA **92:**9450–9454.
44. **Tate, J. J., and T. G. Cooper.** 2003. Tor1/2 regulation of retrograde gene expression in *Saccharomyces cerevisiae* derives indirectly as a consequence of alterations in ammonia metabolism. J. Biol. Chem. **278:**36924–36933.
45. **Tusher, V. G., R. Tibshirani, and G. Chu.** 2001. Significance analysis of microarrays applied to the ionizing radiation response. Proc. Natl. Acad. Sci. USA **98:**5116–5121.
46. **Van Dijken, J. P., J. Bauer, L. Brambilla, P. Duboc, J. M. Francois, C. Gancedo, M. L. Giuseppin, J. J. Heijnen, M. Hoare, H. C. Lange, E. A. Madden, P. Niederberger, J. Nielsen, J. L. Parrou, T. Petit, D. Porro, M. Reuss, N. van Riel, M. Rizzi, H. Y. Steensma, C. T. Verrips, J. Vindelov, and J. T. Pronk.** 2000. An interlaboratory comparison of physiological and genetic properties of four *Saccharomyces cerevisiae* strains. Enzyme Microb. Technol. **26:**706–714.
47. **van Helden, J., B. Andre, and J. Collado-Vides.** 2000. A web site for the computational analysis of yeast regulatory sequences. Yeast **16:**177–187.
48. **Verduyn, C., E. Postma, W. A. Scheffers, and J. P. Van Dijken.** 1992. Effect of benzoic acid on metabolic fluxes in yeasts: a continuous-culture study on the regulation of respiration and alcoholic fermentation. Yeast **8:**501–517.
49. **Wade, J. T., D. B. Hall, and K. Struhl.** 2004. The transcription factor Ifh1 is a key regulator of yeast ribosomal protein genes. Nature **432:**1054–1058.
50. **Zaldivar, J., A. Borges, B. Johansson, H. P. Smits, S. G. Villas-Boas, J. Nielsen, and L. Olsson.** 2002. Fermentation performance and intracellular metabolite patterns in laboratory and industrial xylose-fermenting *Saccharomyces cerevisiae*. Appl. Microbiol. Biotechnol. **59:**436–442.